Molecular Biology of the Cell
Vol. 19, 1439–1449, April 2008

The Tip Growth Apparatus of *Aspergillus nidulans*

Naimeh Taheri-Talesh,* Tetsuya Horio,*† Lidia Araujo-Bazán,‡ Xiaowei Dou,*§ Eduardo A. Espeso,‡ Miguel A. Peñalva,‡ Stephen A. Osmani,* and Berl R. Oakley*

*Department of Molecular Genetics, The Ohio State University, Columbus, OH 43210; †Institute of Health Biosciences, University of Tokushima Graduate School, Tokushima 770-8503, Japan; and ‡Departamento de Microbiología Molecular, Centro de Investigaciones Biológicas, Consejo Superior de Investigaciones Científicas, Madrid 28040, Spain

Submitted May 18, 2007; Revised December 11, 2007; Accepted January 16, 2008
Monitoring Editor: David Drubin

Hyphal tip growth in fungi is important because of the economic and medical importance of fungi, and because it may be a useful model for polarized growth in other organisms. We have investigated the central questions of the roles of cytoskeletal elements and of the precise sites of exocytosis and endocytosis at the growing hyphal tip by using the model fungus *Aspergillus nidulans*. Time-lapse imaging of fluorescent fusion proteins reveals a remarkably dynamic, but highly structured, tip growth apparatus. Live imaging of SYNA, a synaptobrevin homologue, and SECC, an exocyst component, reveals that vesicles accumulate in the Spitzenkörper (apical body) and fuse with the plasma membrane at the extreme apex of the hypha. SYNA is recycled from the plasma membrane by endocytosis at a collar of endocytic patches, 1–2 μm behind the apex of the hypha, that moves forward as the tip grows. Exocytosis and endocytosis are thus spatially coupled. Inhibitor studies, in combination with observations of fluorescent fusion proteins, reveal that actin functions in exocytosis and endocytosis at the tip and in holding the tip growth apparatus together. Microtubules are important for delivering vesicles to the tip area and for holding the tip growth apparatus in position.

INTRODUCTION

Polarized cell growth occurs in most eukaryotic phyla, and it includes a plethora of important phenomena, such as neuronal growth cone extension in animals and pollen tube extension in vascular plants. It is particularly important in filamentous fungi where nearly all growth occurs by hyphal tip extension (reviewed by Momany, 2002). Given that some filamentous fungi are important fermentation organisms, the growth of which is of considerable economic importance, whereas others are serious plant, animal, and human pathogens, there is considerable interest in the mechanisms of tip growth in these organisms.

A great deal of progress has been made in understanding fungal tip growth (summarized by Harris *et al*., 2005; Steinberg, 2007a,b; Riquelme *et al*., 2007), but key questions remain unanswered. There is general agreement that fungal tip growth involves the synthesis of cell wall components in the cell body, the incorporation of these components into vesicles, the transport of these vesicles to the cell tip, the fusion of these vesicles with the plasma membrane in the area of the cell tip (exocytosis) to release their contents, and the cross-linking of the components after release. It is clear that both microtubules and actin microfilaments play important roles in fungal tip growth, but their exact functions are not yet defined. The exact sites of exocytosis and endocytosis also remain to be determined. The positions of the site(s) of exocytosis are particularly important because fungal walls are relatively stiff structures, and once they have formed the shape of the hypha is established. Hyphal shape is thus determined to a very significant extent by where the wall precursors are released from the cytoplasm, i.e., by the positioning of the site(s) of exocytosis. Indeed, in the most current mathematical model of hyphal morphogenesis, the positions of the sites of exocytosis are postulated to be the main determinant of hyphal morphology (Bartnicki-Garcia *et al*., 1989; Bartnicki-Garcia, 1990; Gierz and Bartnicki-Garcia, 2001). The positions of these sites are, in turn, postulated to be governed by the radial movement of vesicles from a vesicle supply center near the tip. Tip growth also likely involves the recycling, by endocytosis, of exocytic vesicle membrane (Fischer-Parton *et al*., 2000; Wedlich-Soldner *et al*., 2000) and proteins involved in fusion with the plasma membrane such as vesicular-soluble *N*-ethylmaleimide-sensitive-factor attachment protein receptor (v-SNAREs) (Pelham, 1999; Lewis *et al*., 2000; Read and Kalkman, 2003). Thus, the positions of the sites of endocytosis are also important.

To begin to answer some of the outstanding questions, we have focused our attention on tip growth in the genus *Aspergillus* and the model species *A. nidulans*. Tip growth in this genus is particularly important because some species (e.g., *A. niger* and *A. oryzae*) produce economically important

This article was published online ahead of print in *MBC in Press* (http://www.molbiolcell.org/cgi/doi/10.1091/mbc.E07–05–0464) on January 23, 2008.

§ Present address: Department of Neurology, Harvard Medical School, VA Boston Healthcare System, 1400 VFW Pkwy., Bldg. 3 RM 2C130, West Roxbury, MA 02134.

Address correspondence to: Berl R. Oakley (oakley.2@osu.edu).

Abbreviations used: ABPA, actin-binding protein A; DMSO, dimethyl sulfoxide; GFP, green fluorescent protein; mRFP, monomeric red fluorescent protein; PCR, polymerase chain reaction; SNARE, soluble *N*-ethylmaleimide-sensitive-factor attachment protein receptor.

Supplemental Material can be found at:
http://www.molbiolcell.org/content/suppl/2008/01/23/E07-05-0464.DC1.html

products, whereas others (e.g., *A. fumigatus*) are serious pathogens, particularly in immune-compromised patients (reviewed by Brookman and Denning, 2000; Latge 2001). Still other species (e.g., *A. flavus*) cause contamination of foods with toxic and carcinogenic aflatoxins (reviewed by Bhatnagar *et al*., 2002).

Information obtained with *A. nidulans* is also likely to be informative with respect to tip growth in other organisms. Although it would be naïve to assume that all tip growth occurs by a single common mechanism, it would be equally naïve to assume that no mechanisms are shared among the different phyla. *A. nidulans* has by most measures the best system for molecular genetic manipulations among organisms that exhibit tip growth (Nayak *et al*., 2006; Szewczyk *et al*., 2006; Osmani *et al*., 2006) (aside from pseudohyphal growth in *Saccharomyces cerevisiae*, which, although interesting in itself, is a slow and atypical form of tip growth), and it is clearly an organism of choice for studying this phenomenon. It is also interesting to note that the situation in *A. nidulans* is remarkably similar to the situation in certain neuromuscular junctions, strongly suggesting that fungal and specialized metazoan cells deal in a similar way with the local excess of membrane and membrane fusion machinery resulting from highly focused, persistent delivery of secretory vesicles to a limited region at the plasma membrane.

We have developed fluorescent fusions of several proteins involved in tip growth, and we have observed their locations by multidimensional time-lapse microscopy in growing hyphae. We have used these fusion proteins in combination with inhibitors of microtubule assembly and filamentous actin assembly to define more precisely the roles of microtubules in tip growth. Our results reveal the existence of a remarkably dynamic but highly structured tip growth apparatus that moves with the growing tip. We are able to define multiple roles for microtubules and actin microfilaments in tip growth and to pinpoint the sites of exocytosis and endocytosis in the tip region. These findings greatly clarify the mechanisms of tip growth and they place significant constraints on permissible models of fungal morphogenesis.

MATERIALS AND METHODS

Fusion Polymerase Chain Reaction (PCR) and Strain Construction

Creation of fusion PCR products for N-terminal tagging of SYNA with green fluorescent protein (GFP) and mCherry and SSOA with GFP was carried out as shown in Supplemental Figure 1. Primers are listed in Supplemental Table 1. In this table, primer synA1-1 (P1) corresponds to primer P1 in Supplemental Figure 1, and so on. Likewise ssoA1-1 (P1) corresponds to P1 in Supplemental Figure 1, except that in this case the fusion PCR construct generated was for creating an N-terminal fusion of SSOA instead of SYNA. For both *synA* and *ssoA*, primers P5 and P6 were different for GFP and mCherry, and they are appropriately labeled. Other primers were used for both GFP and mCherry fusions. PCR enzymes and conditions were as described by Szewczyk *et al*. (2006). The *A. fumigatus pyrG* gene (*AfpyrG*) was used as a selectable marker. With both *synA* and *ssoA*, the promoter region amplified was ~500 base pairs in length. The amplified fragments from the 5′ untranslated region of each gene and from the coding sequence of each gene (Supplemental Figure 1) were ~1000 base pairs. To improve chances that the fusion proteins would be functional, a linker of five glycines and alanines (5 GA) (Yang *et al*., 2004) was incorporated at the C terminus of the GFP and mCherry cassettes such that there was a flexible region between each fluorescent protein and the target protein to which it was fused. The fusion constructs were transformed into strain LO1497 [*fwA*1; *nicA*2; *pyrG*89; *pyroA*4; *nkuA*Δ (*nkuA*::*argB*)]. Correct integration of the transforming fragment was verified by diagnostic PCR and by Southern hybridizations using the method of Oakley *et al*. (1987) with appropriate radioactively labeled fusion PCR fragments as probes. The Southern hybridizations also confirmed that there were no ectopic integrations of the transforming DNA. Multiple transformants were examined by fluorescence microscopy. All *synA* fusions gave the same localization patterns, and all *ssoA* fusions also gave the same localization patterns as each other. A strain expressing GFP-SYNA was designated LO1535, a strain expressing mCherry-SYNA was designated LO1539, and a strain expressing GFP-SSOA was designated LO1545. A strain (LO1548) expressing GFP-SYNA and monomeric red fluorescent protein (mRFP) fused to actin-binding protein A (ABPA-mRFP) was created by crossing LO1535 to a strain expressing ABPA-mRFP (Araujo-Bazán *et al*., 2008). To construct a strain expressing GFP-*tubA* (α-tubulin) and mCherry-SYNA, we crossed LO1539 to LO1028 (*choA*1; *sC*12, *yA*2, GFP-*tubA*). We designated the resulting strain LO1671.

SECC was tagged at its C terminus by using fusion PCR to generate an appropriate transforming fragment (Nayak *et al*., 2006; Szewczyk *et al*., 2006). The *A. fumigatus pyroA* gene (*AfpyroA*) was used as a selectable marker. Primers are listed in Supplemental Table 1. The fusion PCR product was transformed into strain LO1540 [*fwA*1; *nicA*2; *pyrG*89; *pyroA*4; *nkuA*Δ (*nkuA*::*argB*); *AfpyrG*::mCherry-*synA*]. Two transformants were chosen and verified by diagnostic PCR and Southern hybridization. They were given the designations LO2199 and LO2200. The two strains gave identical localization patterns.

In separate experiments, tropomyosin was tagged with GFP at its N terminus and its C terminus. We initially attempted to tag the tropomyosin gene *tpmA* at its normal chromosomal locus. Only a few transformants were obtained, and diagnostic PCR indicated that the transforming fragments had integrated heterologously. This suggested that the tropomyosin GFP fusions might not be fully functional. To circumvent this problem we created, by fusion PCR, constructs to target full-length GFP tropomyosin fusion genes at the *yA* (yellow spore color) locus. For the N-terminal GFP fusion, the transforming fragment consisted of ~1000 base pairs of DNA upstream of *yA*, *AfpyroA* as a selectable marker, the *tpmA* promoter (500 base pairs), GFP, a 5 GA linker, the *tpmA* coding sequence and 1000 base pairs of *yA* downstream sequence. Insertion of this fragment into the *yA* locus deletes *yA* causing the spores produced by the transformant to be yellow. For the C-terminal fusion, the transforming fragment consisted of ~1000 base pairs upstream of *yA* followed by the entire *tpmA* gene with promoter, fused at its 3′ end to a 5GA linker, the GFP coding sequence, *AfpyroA* as a selectable marker; and ~1000 base pairs downstream of *yA*. Correct insertion of this fragment also deletes *yA* causing yellow spore color. LO1540 was used as the recipient strain for transformation. Transformants were verified by diagnostic PCR and Southern hybridizations. We used two transformants carrying N-terminal fusions (LO2264 and LO2265) and two transformants carrying C-terminal fusions (LO2266 and LO2267). Primers are listed in Supplemental Table 1.

Fusion PCR was also used to tag actin at its N terminus with GFP. Three fragments were first amplified using primers actA-P1-actA-P6 (Supplemental Table 1). Primers actA-P1 and actA-P2 were used to amplify the 5′ sequence upstream from the initiation codon and actA-P5 and actA-P6 to amplify the actin sequence. Both reactions used genomic DNA as template for amplification. Primers actA-P3 and actA-P4 amplified GFP. The three fragments were then subjected to fusion PCR using actA-P1 and actA-P6 to amplify the GFP-actin construct. The resulting GFP-actin construct incorporates a linker of Gly-Thr-Ala-Ser-Ala between the GFP and actin sequences. This construct was cotransformed into strain GR5 (*pyrG*89; *wA*3; *pyroA*4) by using *AfpyrG* to select transformants, which were subsequently screened visually for expression of GFP-actin by using standard methodologies. Western blot analysis was carried out to confirm expression of the GFP-actin chimera. The strain used for observation seems to be a diploid that formed spontaneously.

Imaging

Cells were grown and observed using four- or eight-chambered Lab-Tek chambered coverglasses (Nalge Nunc International, Rochester, NY). These consist of plastic growth chambers, with a removable cover, attached to a no. 1 coverslip. Aeration is excellent in these chambers and germlings and hyphae grow vigorously for long periods. Imaging was through the coverslips at the bottom of the chambers. Two IX71 inverted microscopes (Olympus, Tokyo, Japan) were used for imaging. One microscope was initially equipped with a mercury light source and a Uniblitz electronic shutter, a Prior Z-axis drive, an Olympus narrow blue (U-MNB2) filter cube, and a Hamamatsu Orca ER cooled charge-coupled device camera. Subsequently, the Uniblitz shutter was replaced with a Prior shutter and excitation filter wheel. With this arrangement, we used a Semrock GFP/DsRed-2X-A "Pinkel" filter set [459- to 481-nm bandpass excitation filter for GFP and a separate 546- to 566-nm bandpass excitation filter for mCherry, a dual reflection band dichroic (457–480 nm and 542–565 nm reflection bands, 500- to 529 and 584- to 679-nm transmission bands), and dual wavelength bandpass emission filter (500–529 nm for GFP and 584–679 nm for mRFP or mCherry imaging)]. Images were acquired with a 100× 1.3 numerical aperture (N.A.) planfluor objective or 60× 1.42 N.A. planapochromatic objective using Slidebook software (Intelligent Imaging Innovations, Denver, CO) on an Apple PowerMac G4 computer (Apple Computer, Cupertino, CA). The other microscope was equipped with a Hamamatsu ORCA ERAG camera, Prior shutter, Prior excitation and emission filter wheels, and a Semrock GFP/DsRed2X2M-B dual band "Sedat" filter set [459- to 481-nm bandpass excitation filter for GFP and a 546- to 566-nm bandpass excitation filter for mRFP or mCherry, dual reflection band dichroic (457- to 480-nm and 542- to 565-nm reflection bands, 500- to 529-nm

and 584- to 679-nm transmission bands), and two separate emission filters (499–529 nm for GFP and 580–654 nm for mRFP or mCherry)]. Images were acquired using Slidebook software on a PowerMac G5 computer. Because of the greater selectivity between the two wavelengths, the dual filter wheel arrangement was used for most dual wavelength imaging. Some Z-series stacks were deconvolved using Slidebook software. Projections of Z-series stacks and Quicktime movies were made with Slidebook software.

For imaging, strains were grown in liquid minimal medium (6 g/l $NaNO_3$, 0.52 g/l KCl, 0.52 g/l $MgSO_4 \cdot 7H_2O$, 1.52 g/l KH_2PO_4, 10 g/l D-glucose, 1 ml/l trace element solution [Cove, 1966], pH adjusted to 6.5 with NaOH before autoclaving), with appropriate supplements depending on nutritional markers in the strains.

Inhibitor Treatments

Cytochalasin A (Sigma-Aldrich, St. Louis, MO) was stored as a 1 mg/ml stock solution in dimethyl sulfoxide (DMSO), and latrunculin B (Sigma-Aldrich) was stored as a 10 mg/ml stock in DMSO. In time-lapse solvent-only control experiments, we found that if small amounts of DMSO were added to our observation chambers, the DMSO sank to the bottom of the chamber to the cells we were observing and it inhibited growth. To circumvent this problem, 300 μl of growth medium was removed from the observation chamber and replaced with 300 μl of growth medium into which an appropriate volume of inhibitor stock solution had been mixed. Using this procedure, growth was not inhibited at all in repeated (>10) DMSO-only control experiments. Cytochalasin A was used at a final concentration of 1.0 μg/ml (2.1 μM), and latrunculin B was used at a concentration of 40 μg/ml (100 μM). It is worth noting that we have used a much lower concentration of cytochalasin A than was used by Torralba *et al*. (1998). One of us has found that *A. nidulans* apparently degrades cytochalasin A such that low concentrations of cytochalasin A inhibit growth, but eventually growth inhibition ends. If low concentrations of cytochalasin A are added at intervals, growth inhibition is maintained (Oakley, unpublished data). Cytochalasin A is thus an effective inhibitor at low concentrations, but it is probably destroyed by *A. nidulans*. Regardless, the low concentration we used was sufficient to disassemble F-actin and completely stop growth. We prefer to use lower concentrations because they are less likely to have secondary effects. Benomyl was stored and used as reported previously (Horio and Oakley, 2005). For washout experiments, the culture medium containing the inhibitor was gently removed from the observation chambers with a transfer pipette and replaced with medium without inhibitor. This was repeated three to four times.

RESULTS

Localization and Imaging of Actin and Tropomyosin in Living A. nidulans Cells

Polarized growth in *A. nidulans* requires actin (Torralba *et al*., 1998), and its location and dynamics are likely to be a key to tip growth. Actin has been visualized in fixed *A. nidulans* by immunofluorescence microscopy (Harris *et al*., 1994, 1997; McGoldrick *et al*., 1995; Torralba *et al*., 1998; Cheng *et al*., 2001), but it has not been imaged in living cells. We consequently constructed a strain expressing a fusion of GFP to the N terminus of actin (*A. nidulans* contains a single actin gene; Fidel *et al*., 1988). The strain was healthy, growing, and conidiating normally at all temperatures, and the results with the anti-actin agents cytochalasin A and latrunculin B (see below) confirmed molecular biological evidence that the observed fluorescence was indeed due to actin.

The most conspicuous actin-containing structures are actin patches, and we were able to determine by analyzing Z-series stacks that they are located predominantly, and probably exclusively, at the hyphal cortex. In swollen isotropically growing conidia, they are simply scattered around the cortex. At the time of polarity establishment a few patches become associated with the germ tube emergence site (Figure 1A). In germlings and mature hyphae, they are concentrated near the hyphal tip as was observed previously (Harris *et al*., 1994; Torralba *et al*., 1998), but we found that the pattern changes as the germlings grow into mature hyphae. In germlings, the patches are simply concentrated near (but not restricted to) the apex (Figure 1B). For brevity, we use the term "tip" for the general tip region and "apex" for the extreme tip of the cell. As germ tubes extend and rounds of asymmetrical cell divisions occur, tip growth accelerates approximately fivefold (Horio and Oakley, 2005), and this is accompanied by a reorganization of actin patches into a prominent ring or collar 1–2 μm behind the hyphal apex (Figure 1C). Actin patches are generally not present

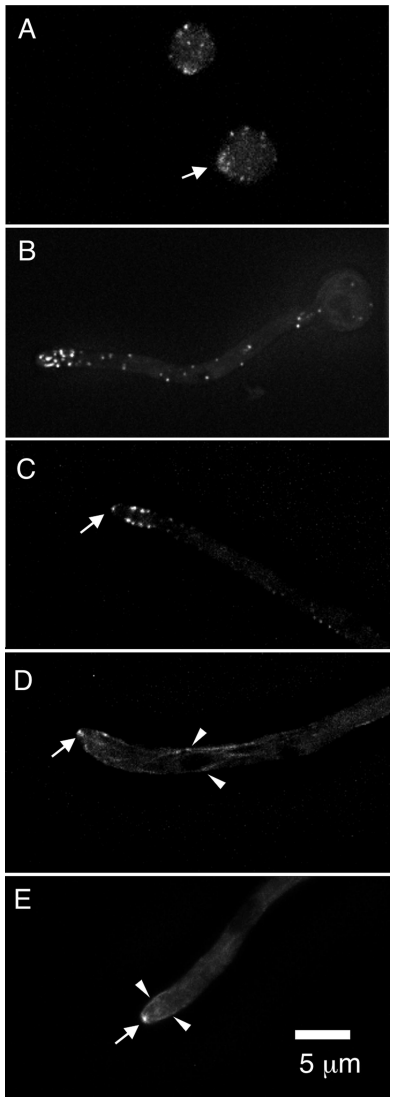

Figure 1. GFP-actin and GFP-tropomyosin localization. (A) A maximum intensity projection of a Z-series stack from a set of time-lapse images showing actin in two swollen conidia (asexual spores). In the lower conidium, the actin has accumulated (arrow) at a site at which germ tube emergence is occurring. (B) A maximum intensity projection of a Z-series stack through a germling. The remnant of the swollen conidium is visible at the right. GFP-actin patches are clustered near the tip and scattered behind the tip. (C) A single focal plane image of a rapidly growing tip cell. Because it is a single focal plane image rather than a projection, the cortical location of the actin patches is clear. Note the single actin spot at the hyphal apex (arrow). Such spots are presumably present in germlings, but they are difficult to distinguish among the actin patches. (D and E) Localization of N-terminally tagged tropomyosin at a growing hyphal tip. Tropomyosin localizes to the Spitzenkörper (arrows) and to microfilaments (some of which are designated with arrowheads). Microfilaments pass near the plasma membrane and extend pass the region in which the collar of actin patches is found. Two such microfilaments are shown in E (arrowheads). All panels are the same magnification and were deconvolved to reduce background fluorescence.

anterior to this collar, but they are present at lower densities posterior to the collar.

In addition to the actin patches, hyphal tips (both germlings and hyphal tip cells) contained a single actin spot, fainter than the actin patches, at the apex (Figure 1C) at the position of the Spitzenkörper (discussed below). This structure has not been revealed previously by immunofluorescence microscopy, but a meshwork of actin filaments has been seen in this position by freeze-substitution electron tomography (Hohmann-Marriott *et al*., 2006). We were not able to visualize extended actin filaments (cables). In previous studies, these have been difficult to image, but they have been visualized by immunofluorescence (Harris *et al*., 1994; Araujo-Bazán *et al*., 2008) and by using a GFP-tropomyosin fusion (Pearson *et al*., 2004). As reported previously (Harris *et al*., 1994; Torralba *et al*., 1998; Cheng *et al*., 2001), actin was also associated with forming septa (data not shown).

Time-lapse microscopy revealed that the actin patches were highly dynamic (see Supplemental Video1.mov). They moved both toward and away from the apex and formed and disappeared rapidly. Indeed, they were sufficiently dynamic that it was difficult to follow them long enough to determine their life span with precision. It is safe to say, however, that the average life span of an actin patch at 25°C is a few seconds, certainly less than a minute. Importantly, as the hyphal tip grew, the ring of actin patches stayed approximately the same distance from the apex. This implies that although individual actin patches are highly dynamic, their movement is somehow coordinated with tip growth or that the hyphal apex and the ring of patches are physically linked.

A tropomyosin (*tpmA*) GFP fusion has been used to image actin cables (Pearson *et al*., 2004), and because we were unable to image cables with our GFP-actin fusion, we constructed both N-terminal and C-terminal tropomyosin GFP fusions. We found that tropomyosin was concentrated near the apex and at forming septa as reported previously (Pearson *et al*., 2004). Deconvolution of *z*-axis series stacks revealed, additionally, that the tropomyosin at the apex is mainly concentrated in the Spitzenkörper and in cables extending back from the apex (Figure 1, D and E). The cables often ran very near the plasma membrane at the tip (Figure 1E), and there was sometimes brighter tropomyosin fluorescence in this area, perhaps reflecting multiple cables very close to each other. As expected, tropomyosin did not seem to be a component of actin patches, but actin/tropomyosin cables did run very close to plasma membrane in the region of the collar of actin patches.

Localization of a Vesicular SNARE, a Target SNARE, and the A. nidulans Homologue of Actin Binding Protein 1 in Living Cells

A key aspect of polarized hyphal growth is the apical release of cell wall biosynthetic and remodeling enzymes and cell wall precursors from the cytoplasm by exocytosis. This is critical for the mechanics of hyphal growth, and it is postulated to be critical for the establishment of the hyphal shape (Bartnicki-Garcia *et al*., 1989; Bartnicki-Garcia, 1990; Gierz and Bartnicki-Garcia, 2001). Exocytosis presumably creates an excess of membrane at the tip that must be internalized by endocytosis (Read and Kalkman, 2003). To understand how tips grow, it is thus necessary to know where exocytosis and endocytosis occur. In *S. cerevisiae*, actin patches are known to be sites of endocytosis (reviewed by Engqvist-Goldstein and Drubin, 2003). A prototypic component of these endocytic patches is actin binding protein 1 (Engqvist-Goldstein and Drubin, 2003; Kaksonen *et al*., 2003, 2005; Huckaba *et al*., 2004; Sun *et al*., 2006). The gene encoding the *A. nidulans* homologue of actin binding protein 1 has been identified by Araujo-Bazán *et al*. (2008) and designated *abpA*. We used an mRFP fusion to the C terminus of the *abpA* product (here designated ABPA) (Araujo-Bazán *et al*., 2008) to observe its location in living cells, and we found that its location was indistinguishable from that of actin (with a collar of ABPA-mRFP behind the tips of rapidly growing hyphae; Figure 2, B and C) except that we did not observe an ABPA-mRFP spot at the hyphal apex. The fact that the collar of patches contains both actin and ABPA is consistent with them being endocytic sites. Additional evidence that they are endocytic patches has been obtained by Araujo-Bazán *et al*. (2008).

The polarized delivery of secretory vesicles to the plasma membrane involves mechanisms by which SNARE proteins in the membrane of secretory vesicles are efficiently recycled to reenter the exocytic pathway. In budding yeast, the SNC1/SNC2 pair of R-SNARE (a form of v-SNARE) paralogues encodes fungal homologues of mammalian synaptobrevin proteins. Snc1p/Snc2p are exocytic SNAREs involved in the fusion of secretory vesicles with the plasma membrane (Protopopov *et al*., 1993). Snc1p is recycled from the plasma membrane by endocytosis and subsequently retrieved to the Golgi from an early endosomal compartment (Lewis *et al*., 2000). An *A. nidulans* SNC1 homologue should thus be an excellent marker for both exocytosis and endocytosis at the growing tip.

The yeast Qa SNARE Sso1p is a target (t)-SNARE) that serves as a membrane-specific tag in the docking of transport vesicles to the plasma membrane (Aalto *et al*., 1993). Sso1p is not a substrate of the endocytic recycling pathway, and its distribution in the plasma membrane is not significantly polarized in yeast (Valdez-Taubas and Pelham, 2003). It is thus likely to be an excellent marker for the plasma membrane. The *A. nidulans* single *SNC1* and *SSO1* homologues are AN8769.3 and AN3416.3, respectively (using the Broad Institute gene designations at http://www.broad.mit.edu/annotation/genome/aspergillus_nidulans/Home.html). We now designate the *A. nidulans SNC1* homologue *synA* and the *SSO1* homologue *ssoA*, by using standard *A. nidulans* nomenclature, and we designate the products of these genes SYNA and SSOA. (*sncA* is a more obvious designation for the *SNC1* homologue, but this designation has been used for another *A. nidulans* gene.) We note that AN3416.3 is incorrectly annotated in the genome database. The correct gene structure was determined using cDNA sequence coverage available in expressed sequence tag databases.

To observe SYNA and SSOA at the tips of living hyphae, we wanted to generate strains expressing GFP and mCherry protein fusions of these proteins by using gene replacements. Functional tagging of SNAREs requires attachment of the fluorescent proteins to their N termini because SNAREs usually contain a single C-terminal transmembrane domain such that their C termini are in or very near the membrane in which they are embedded (Ungar and Hughson, 2003). However, we wanted to retain the endogenous promoters for these genes to avoid any problems arising from nonphysiological levels of expression. Although fusion PCR allows rapid production of transforming fragments, procedures to date involve C-terminal tagging of the target proteins (Yang *et al*., 2004). We consequently developed a novel five-piece fusion PCR procedure that allowed us to make appropriate transforming constructs with N-terminal fluorescent protein fusions expressed under the control of the normal promoters (discussed in *Materials and Methods*

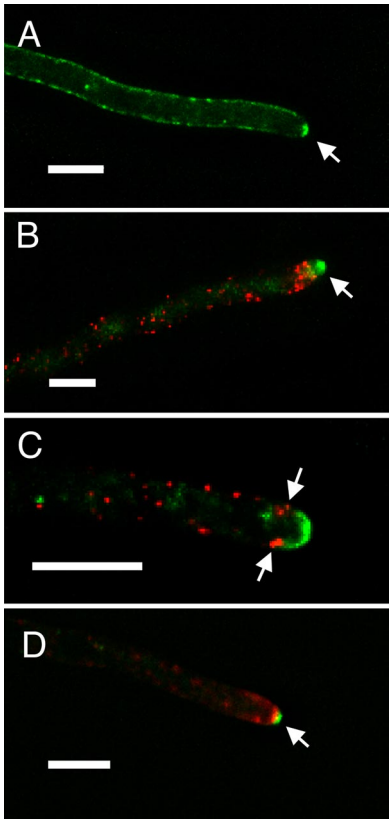

Figure 2. Localization of SSOA, SYNA, ABPA, and SECC in living cells. (A) Hyphal tip cell expressing GFP-SSOA. The image is from a Z-series stack (0.5-μm vertical spacing between captures) that has been deconvolved. The image is a maximum intensity projection image of three consecutive sections. SSOA is predominantly at the plasma membrane, and there is a region of greater SSOA concentration at the hyphal apex (arrow) and a region of reduced concentration immediately posterior to the apical SSOA patch. The SSOA is not evenly distributed through the plasma membrane but has a patchy or punctate distribution. (B) ABPA-mRFP (red) and GFP-SYNA (green). It is a maximum intensity projection of a deconvolved Z-series stack (0.5-μm vertical spacing between captures) through the entire hyphal tip cell. The threshold for the green channel was chosen such that the Spitzenkörper is clear (arrow), but the GFP-SYNA at the membrane anterior to the ABPA patches is less clear. The ABPA patches form a collar around the hypha behind the apex and the Spitzenkörper. (C) A single optical section of a hyphal tip cell expressing GFP-SYNA and ABPA-mRFP. The Spitzenkörper was not particularly prominent in this cell, and it was mainly located in a different optical plane. This allows the SYNA localization at the plasma membrane to be seen clearly. SYNA is at the plasma membrane between the apex and the collar of ABPA patches. In this focal plane, four ABPA patches from the collar are visible (arrows). There is a particularly prominent internal SYNA-containing structure that seems too large to be a vesicle immediately posterior to the top patches. SYNA-containing structures varied considerably in size, and we speculate that this could be a Golgi apparatus or endosome. The cortical location of the ABPA patches is evident near the tip. The hypha, however, is at a slight angle relative to the plane of optical section, and this makes some of the ABPA patches seem internal, although they are, in fact, cortical. The ABPA patches further away from the tip are actually at the surface of the cell nearest the reader. (D) mCherry-SYNA (red) and SECC-GFP (green). SECC, an exocyst component, localizes to the apex (arrow). Bars, 5 μm.

and shown in Supplemental Figure 1). These constructs were transformed into an *A. nidulans* strain and the correct gene replacement events were verified by diagnostic PCR and Southern hybridizations (data not shown). The GFP and mCherry fusions of each protein gave the same localization patterns as each other and the strains carrying the fusions were healthy, showing no evidence of reduced growth at any temperature or alteration of conidiation. Multiple transformants were observed for each fusion, and they gave the same localization pattern. The following conclusions are based on observations of many single-time point Z-series stacks and time-lapse data sets.

The fluorescence signal of GFP-SSOA was weaker than that of our other fluorescent fusion proteins. As expected, it localized to the plasma membrane (Figure 2A), but the fluorescence was not completely uniform in the membrane; rather, it was patchy. This is in marked contrast with the uniform localization of GFP-Sso1 in the *S. cerevisiae* plasma membrane. Interestingly, we generally found a small region of higher concentration (i.e., brighter GFP fluorescence) at the hyphal apex and a region of lower concentration immediately behind the apical SSOA patch (Figure 2A).

The GFP-SYNA fusion protein would be expected to localize to secretory vesicles and during exocytosis, as the vesicles fuse with the plasma membrane, GFP-SYNA should become incorporated into the plasma membrane. SYNA was, indeed, found at dots in the hypha, many of which undoubtedly correspond to such vesicles. (Note that there are also some larger SYNA-containing structures that could correspond to larger endosomal compartments; see below.) The Spitzenkörper ("apical body" or "tip body" in English) is an incompletely defined structure observed at the tips of growing hyphae in many fungi that is thought to be critically important for tip growth (recently reviewed by Harris *et al*., 2005), and vesicles are a major component of the Spitzenkörper. Thus, one would expect GFP-SYNA to reveal the Spitzenkörper, and, indeed, in rapidly growing hyphal tips a vesicle cluster or Spitzenkörper was visible (Figure 2B). Four-dimensional image sets (Z-series captured over time) revealed that the size and brightness of the Spitzenkörper fluctuated to some extent as hyphae grew. The Spitzenkörper was at the apex, and as it shifted to one side or another, the direction of hyphal growth followed (Supplemental Video2.mov). It is interesting to note, however, that in germlings GFP-SYNA localization gave no evidence for a Spitzenkörper.

Most interesting was the location of GFP-SYNA at the hyphal tip. Z-series stacks revealed that SYNA was located at the plasma membrane in a hemisphere extending from the hyphal apex back to the ring of actin/ABPA patches (Figure 2C). Although the resolution of light microscopy does not allow one to determine whether SYNA is embedded in the membrane or just in contact with the membrane, the biology of R-SNARES argues strongly that SYNA is a component of the plasma membrane in this region. For example, in *S. cerevisiae*, an epitope-tagged version of Snc1 has previously been shown to be present largely in the plasma membrane (Protopopov *et al*., 1993; Lewis *et al*., 2000; Valdez-Taubas and Pelham, 2003).

It is important to note that in *A. nidulans* SYNA was not detected at the plasma membrane posterior to the collar of actin/ABPA patches. This indicated that exocytosis occurs predominantly, and perhaps exclusively, anterior to this collar. To obtain a clearer picture of the site(s) of exocytosis, we identified, tagged and imaged the *A. nidulans* homologue of the *S. cerevisiae SEC3* gene. Sec3p, a component of the exocyst, is a landmark for the site of polarized exocytosis (Finger *et al*., 1998). A blast search of the *A. nidulans* database revealed a single, unambiguous *SEC3* homolog (e value

$2e^{-27}$), AN0462.3 (Broad database designation). We designate this gene *secC* and its product SECC. We created a fusion of GFP to the C terminus of SECC, and we found that it localized consistently to a small region at the plasma membrane at the apex, immediately anterior to the Spitzenkörper (Figure 2D). This indicates that exocytosis occurs at, and is probably restricted to, a very small region at the apex of the growing hypha.

From multiple time-lapse image sets, it is clear that the actin at the apex, the Spitzenkörper, the region of SYNA at the membrane, SECC, and the actin/ABPA patches all move forward together as the tip grows and constitute some form of complex (Supplemental Video2.mov). For brevity, we call this the "tip growth complex."

Effects of the Anti-Actin Agents Cytochalasin A and Latrunculin B on Actin Patches, Cables, and the Tip Growth Complex

To clarify the role of actin in tip growth, we treated hyphae with cytochalasin A, which has been shown to depolymerize filamentous actin (F-actin) in *A. nidulans* (Torralba *et al*., 1998), and with latrunculin B, another F-actin depolymerizing agent. The results obtained with the two compounds were essentially identical. The subapical actin patches and the actin spot at the hyphal apex disappeared immediately (<5 min). Tip growth stopped almost immediately (<10 min), and the hyphal tips bulged slightly (Figure 3, Supplemental Video3.mov and Video4.mov, and Supplemental Figure 2).

Cytochalasin A and latrunculin B effects on hyphae expressing ABPA-mRFP and GFP-SYNA were similar but not identical to each other. With cytochalasin A, the ABPA patches did not disappear but they became delocalized. They initially collapsed toward the tip of the hypha (Figure 4D). Subsequently, they remained cortical but became distributed, apparently randomly, through the cortex (Figure 4G). Imaging of GFP-SYNA revealed that the vesicular cluster that is integral to the Spitzenkörper generally disappeared rapidly. Occasionally, however, it drifted away from the hyphal apex and remained visible for a few minutes before disappearing (Figure 4E). This seems to indicate that this cluster has some degree of structural integrity and that its localization at the apex is F-actin dependent. GFP-SYNA remained at the plasma membrane near at the hyphal tip, but, notably, the membrane area to which it localized increased with time (Figure 4H).

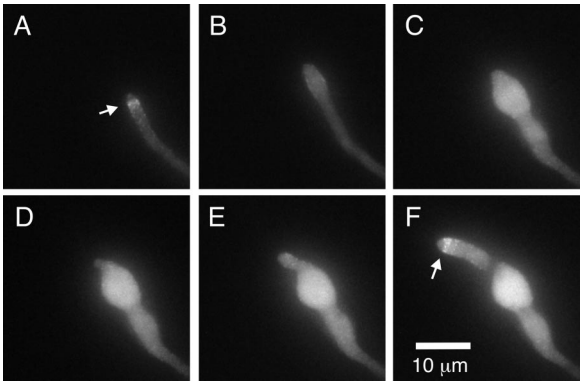

Figure 3. Cytochalasin A treatment and washout in a strain expressing GFP-actin. These are maximum intensity projections of Z-series stacks from a time-lapse data set (see Supplemental Video3.mov). (A) GFP-actin localization in a hyphal tip immediately before cytochalasin A addition. The collar of actin patches is visible (arrow). (B) Fifteen minutes after cytochalasin A addition and immediately before cytochalasin A washout. Actin patches have dissolved, and the tip has swollen. (C) Seventy minutes after cytochalasin A washout. The tip has swollen further. (D) Eighty minutes after cytochalasin A washout. A hyphal tip has emerged. (E) Ninety minutes after cytochalasin A washout. The hyphal tip has begun to extend. (F) One hundred minutes after cytochalasin A washout. A collar of actin patches has reformed (arrow). The new hypha is larger in diameter than the hypha before cytochalasin A treatment.

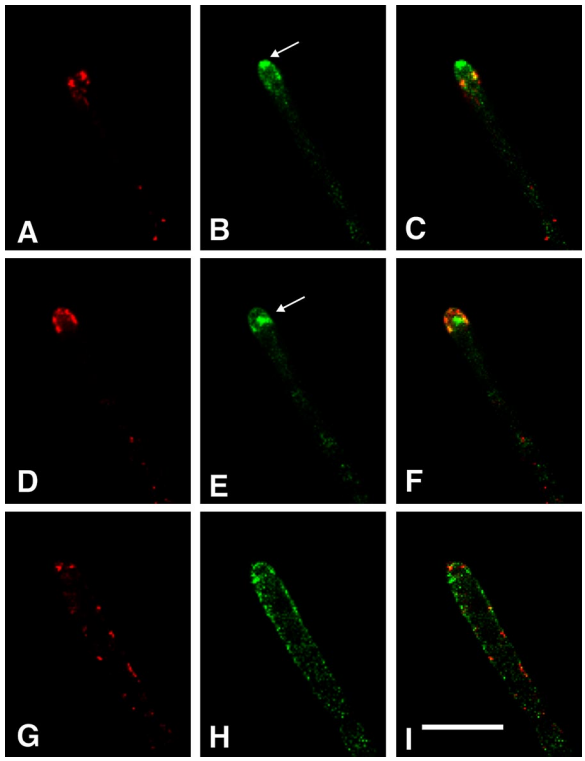

Figure 4. GFP-SYNA and ABPA-mRFP in a cytochalasin A-treated hypha. Each frame is a single focal plane image from deconvolved Z-series stacks taken as part of a time-lapse series. A, D, and G show ABPA-mRFP. B, E, and H show GFP-SYNA. C, F, and I are color composites. (A–C) A hyphal tip immediately before cytochalasin A addition. The Spitzenkörper is designated with an arrow in B. GFP-SYNA is in the Spitzenkörper, and vesicles are in the hypha (fainter) and at the plasma membrane between the hyphal apex and the collar of ABPA patches. (D–F) The same hyphal tip 5 min after cytochalasin A addition. The vesicular cluster of the Spitzenkörper has floated back from the hyphal apex (arrow in E), and the ABPA-mRFP patches have moved to the tip area (D). (G–I) The same hypha 1 h after cytochalasin A addition. GFP-SYNA now occupies a larger area of the plasma membrane at the tip region (H), although the fluorescence signal is weaker, indicating less GFP-SYNA per unit area. mRFP-ABPA is now apparently randomly distributed in the cortex (G). Bar (I), 10 μm.

With latrunculin B treatment, ABPA patches did not immediately disappear but, after initial delocalization of the patches, a portion of ABPA-GFP localized to the cytosol apparently at the expense of the cortical patches, which became less apparent. Some ABPA-mRFP localized to the membrane in the swollen tip area as uniform fluorescence rather than patches. GFP-SYNA localization was similar to that in cytochalasin A-treated cells (Figure 5 and Supplemental Video4.mov).

The effects of both cytochalasin A (Figure 3 and Supplemental Video3.mov and Video5.mov) and latrunculin B (Supplemental Video 6.mov) were reversible, although the

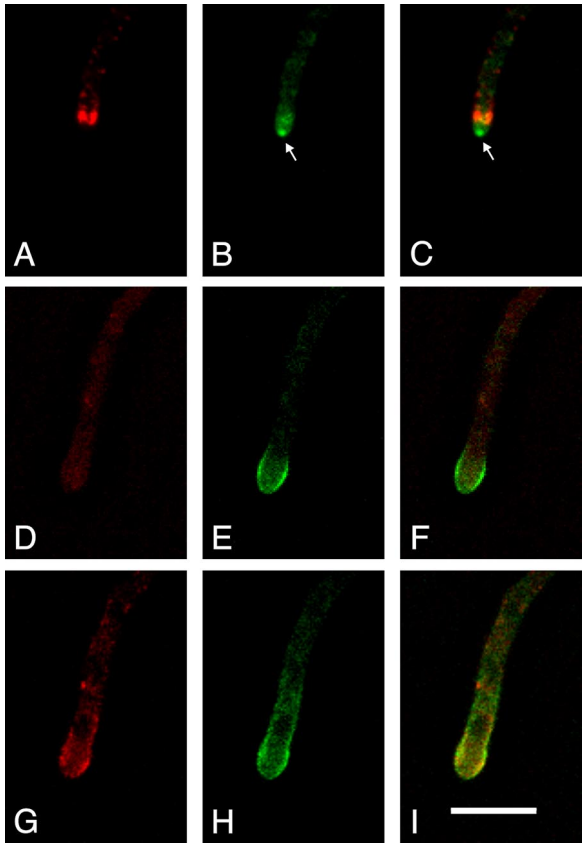

Figure 5. GFP-SYNA and ABPA-mRFP in a latrunculin B treated hypha. Each frame is from deconvolved Z-series stacks taken as part of a time-lapse series (see Supplemental Video4.mov). A, D, and G show ABPA-mRFP. B, E, and H show GFP-SYNA. C, F, and I are color composites. (A–C) A single focal plane image of a hyphal tip taken 10 min before latruculin B addition. The Spitzenkörper is designated with an arrow. GFP-SYNA is in the Spitzenkörper and in vesicles near the tip and further back in the hypha. In this case, there are so many vesicles in the vicinity of the tip that it is difficult to distinguish the GFP-SYNA at the membrane in the region between the apex and the ABPA patches from the vesicles. (D–F) A single focal plane image of the same hyphal tip 15 min after latrunculin B addition. The tip has bulged and the ABPA-mRFP patches have dispersed. The GFP-SYNA at the membrane is now clearly visible because there are fewer vesicles in the tip area and it occupies a larger area than before latrunculin B addition. (G–I) A projection of two consecutive Z-series images of the same hypha 60 min after latrunculin B addition. GFP-SYNA now occupies a larger area of the plasma membrane at the tip region (H), although the fluorescence signal is weaker, indicating less GFP-SYNA per unit area. Bar (I), 10 μm.

reversal was not rapid. When these compounds were washed out of the culture chambers, normal growth and organization of actin, ABPA, and SYNA were restored, although restoration of tip growth often took >1 h. When cytochalasin A or latrunculin B was washed out, the swollen tip exhibited additional swelling, and then one or more hyphal tips eventually emerged and extended. (Figure 3 and Supplemental Video3.mov, Video5.mov, and Video6.mov). The hyphal tips that emerged were often larger than those seen before treatment.

We also observed the effects of cytochalasin A on actin cables by using our GFP-tropomyosin fusion. As expected, actin cables disassembled rapidly upon addition of cytochalasin A, and they were undetectable 5 min after cytochalasin A addition.

Effects of Antimicrotubule Agent Benomyl on Tip Growth and the Tip Growth Complex

Horio and Oakley (2005) have studied the effects of the antimicrotubule agent benomyl on tip growth. From these and previous studies (e.g., Oakley and Morris, 1981), it is clear that benomyl is an excellent antimicrotubule agent in *A. nidulans*. It causes rapid microtubule disassembly (all microtubules disassemble in <10 min after addition to the culture chamber), it is rapidly reversible (microtubules begin to reassemble in <5 min after benomyl is washed out), and it is quite specific for microtubules (Oakley and Morris, 1981). Treatment with benomyl caused a dramatic reduction in tip growth rate but not a complete stoppage of growth (Horio and Oakley, 2005). It was also noted that benomyl treatment led to growth away from the tip. Side branches were sometimes formed, and there were sometimes bulges in the hyphae.

We have extended these observations with time-lapse microscopy documenting the effects of benomyl on tip growth and the localization of actin, ABPA and SYNA. We first verified that benomyl was depolymerizing microtubules as expected using a GFP–α-tubulin fusion (Horio and Oakley, 2005). After benomyl addition, as noted previously, growth of the tip slowed. In addition, side branches often formed in the tip cell, whereas side branches never formed in the tip cells of controls. In benomyl, growth was often highly curved both at the hyphal tip and at the tips of side branches (Figure 6).

When hyphae expressing GFP-actin were treated with benomyl, the actin patches remained visible as expected, but their distribution often changed significantly over time. The change in distribution was not identical among treated hyphae, but there were some common themes. In most hyphae, the tip growth apparatus, as imaged by GFP-actin or ABPA-mRFP and GFP-SYNA, was eventually displaced from the tip. In some cases, the displacement was rapid, whereas in other cases the tip growth apparatus remained intact and in place for as much as an hour (Supplemental Video7.mov). In some cases when the tip growth apparatus was displaced from the tip, growth of one or more side branches started almost immediately, and at least a rudimentary tip growth apparatus was present at the growing side branches. In these cases, the tip growth apparatus was often less organized than in rapidly growing tip cells and resembled that of germlings. In other cases, the tip growth apparatus disassembled and did not reform during the observation period of >1 h. The effects of benomyl were rapidly reversible. We found that within 10 min of benomyl washout, normal, directional tip growth resumed (Figure 6), and it was accompanied by the typical arrangement of actin/ABPA patches (Figure 6) and SYNA (data not shown) seen at rapidly growing tips.

DISCUSSION

A. nidulans Possesses a Dynamic but Structured Tip Growth Apparatus

Our results reveal that, in rapidly growing hyphae, the Spitzenkörper, the ring of actin/ABPA patches, the region of SYNA at the plasma membrane, SECC, and the actin spot at the apex are maintained in a consistent spatial relationship with each other and with the hyphal apex. Published data suggest that the polarisome and a region of spingolipids also maintain a consistent spatial relationship with these struc-

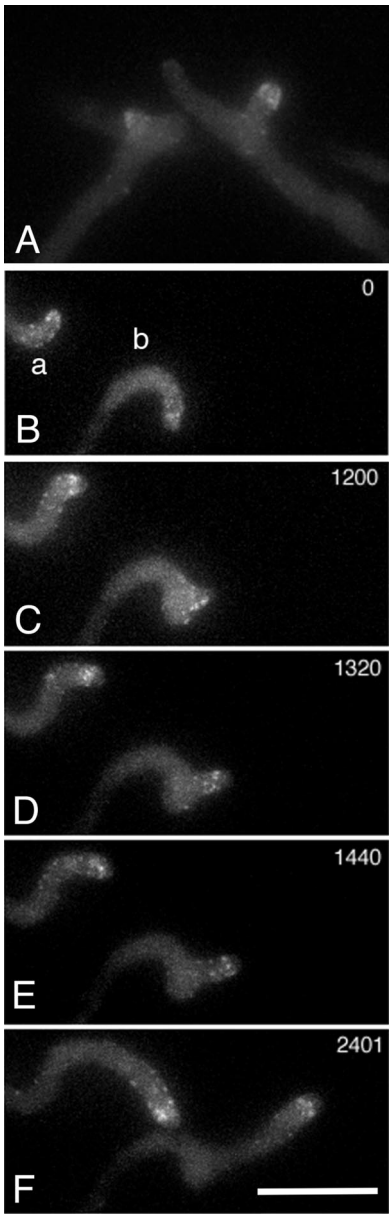

Figure 6. Benomyl treatment and recovery in a strain expressing GFP-actin. (A) Abnormal branching after benomyl treatment. Lateral branching does not normally occur in the tip cell. (B–F) Recovery of a different pair of hyphae after benomyl washout. The time after benomyl washout (in seconds) is given at the upper right of each panel. At T = 0, the hyphal tips display obvious curvature. Over time, the actin patches become more organized and the hyphal tip displays more rapid and straighter growth. Bar (F), 10 μm.

tures and the apex (Sharpless and Harris, 2002; Harris *et al*., 2005; Li *et al*., 2006). We suggest that rather than thinking of these structures as separate entities, it is useful to think of them as components of a highly structured tip growth apparatus in which the positions of individual components are precisely maintained to achieve efficient tip growth. Although highly structured, this apparatus is also highly dynamic in two senses. First, it moves as the tip grows. The tip shown in Supplemental Video2.mov, for example, grew at ~1 μm/min and the entire apparatus thus had to move forward at this rate while maintaining the spatial relationships of its components. Second, individual components are highly dynamic. For example, the actin/ABPA patches are extremely dynamic. They move forward and backward and appear and disappear with a half-life of <1 min, similar to their behavior in *S. cerevisiae* (Smith *et al*., 2001; Kaksonen *et al*., 2003). Although individual patches are quite dynamic, the position of the collar as a whole is relatively stable. There must be a mechanism for establishing the collective position of the patches while allowing individual patches to move forward and backward, to assemble and to disappear. The formin SEPA, a component of the polarisome, is also dynamic (Sharpless and Harris, 2002), exocytic vesicles are dynamic, and, indeed, it is likely that many other components of the tip growth apparatus will be found to be dynamic.

Our data strongly indicate that the tip growth apparatus is held together by actin cables. First, the actin cables are perfectly positioned to connect the components of the tip growth apparatus. Second, treatment with cytochalasin A or latrunculin B caused the cables to disassemble and the components of the tip growth apparatus to lose their spatial relationship. Moreover, the tip growth apparatus fell apart in an interesting way after treatment with actin depolymerizing agents. After treatment, the vesicular cluster of the Spitzenkörper sometimes drifted away from the apex before it disassembled, and this indicates that F-actin plays a role in tethering this cluster to the apex as well as being essential for maintaining the integrity of the Spitzenkörper. After treatment, actin/ABPA patches also became delocalized. This was true for cytochalasin A treatments and latrunculin B treatments, but it was more obvious with cytochalasin A treatments because the ABPA patches were visible for longer after treatment. It is worth noting that actin cables interact with endocytic patches, and they are involved in their movement in *S. cerevisiae* (Huckaba *et al*., 2004), so it is not surprising that actin cables seem to be involved in the positioning of the actin/ABPA patches in *A. nidulans*. Finally, it is also worth noting that actin is essential for the localization of SEPA (Sharpless and Harris, 2002), another component of the tip growth apparatus.

The organization of the tip growth apparatus correlated with the tip growth rate. In *A. nidulans*, conidia germinate, and after a short period of isotropic growth, they form germ tubes. Repeated rounds of nuclear division followed by asymmetric cell division lead to the formation of tip cells with many nuclei that grow much more rapidly than germlings (discussed by Horio and Oakley, 2005). As discussed, hyphal tip cells have very structured tip growth apparatuses. We have found, however, that in germlings, which have relatively slow growth rates, there is no obvious, structured tip growth apparatus. Actin/ABPA patches are simply clustered near the tip, and there is no obvious Spitzenkörper. This suggests that the tip growth apparatus is not strictly required for growth, but that it has been developed by fungi to allow the impressively rapid growth rates they exhibit.

Exocytosis, Endocytosis, and Hyphal Morphogenesis

Exocytosis and endocytosis are essential for tip growth, and one can think of the tip growth apparatus as simply a machine for delivering exocytic vesicles to the correct place and for recycling membrane and other vesicular components. The sites of exocytosis are also postulated to determine the shape of the growing hypha (Bartnicki-Garcia *et al*., 1989; Bartnicki-Garcia, 1990; Gierz and Bartnicki-Garcia, 2001); thus, it was of particular interest to follow membrane trafficking by using fusion proteins of the synaptobrevin homologue SYNA, an exocytic SNARE (Gerst, 1997). Given

that SYNA is a member of a family of prototypic markers for exocytic vesicles (Protopopov *et al*., 1993; Gerst, 1997; David *et al*., 1998), it is strongly predicted to be a component of exocytic vesicles that becomes a transient component of the plasma membrane when exocytosis occurs, and then is recycled by endocytosis. Completely consistent with these predictions, we have found that SYNA localizes to small dots in the cytoplasm, to the Spitzenkörper and to the plasma membrane at the hyphal apex. The localization at the plasma membrane survives treatments with cytochalasin A and latrunculin B, which is consistent with the notion that SYNA is embedded in the plasma membrane rather than just being in vesicles near the membrane. The fact that the SYNA association with the plasma membrane was only seen in a more or less hemispherical region between the apex and the collar of actin/ABPA patches indicates to us that most, perhaps all, exocytosis occurs in this region. The vesicle density in the tip region is too high to allow us to observe individual exocytotic events so we cannot define the sites of exocytosis more precisely using GFP-SYNA. We have, however, tagged SECC, the homologue of a highly conserved exocyst component, and it localizes to a small region of the plasma membrane at the apex. These data in combination argue very strongly that the great majority of exocytosis occurs in a small region anterior to the collar of actin/ABPA patches, and it probably occurs in the small region defined by SECC-GFP localization. These data do not seem to be particularly supportive of the most current models for morphogenesis in which hyphal shape is determined by radial movement of vesicles from the Spitzenkörper (Bartnicki-Garcia *et al*., 1989; Bartnicki-Garcia, 1990; Gierz and Bartnicki-Garcia, 2001). Such models predict that exocytosis would occur over a broader region than our data indicate.

The fact that there is a great deal of SYNA at the Spitzenkörper is supportive of the widely held notion that the Spitzenkörper is a vesicle supply center, a place where exocytic vesicles containing wall precursors accumulate before fusion with the plasma membrane. It is worth noting, however, that we find no evidence that the Spitzenkörper is present in short germlings. Thus, the Spitzenkörper may be an adaptation for rapid growth rather than a requirement for growth or for the establishment of hyphal shape.

Polarized growth in *A. nidulans* clearly requires F-actin (Torralba *et al*., 1998; this study), and an obvious model is that the docking of vesicles with the plasma membrane at the tip requires movement of vesicles along F-actin cables. Our tropomyosin localization data reveal that F-actin cables are well positioned to move vesicles to the Spitzenkörper. Our data on localization of SYNA after cytochalasin A and latrunculin B treatments are also consistent with this model in that we find no evidence of polarized exocytosis after actin depolymerization. We sometimes noted a slight bulging of tips after cytochalasin A and latrunculin B treatment (Figure 5), and it is possible, consequently, that some nonpolarized exocytosis can occur in the absence of actin. It has been shown biochemically, however, that cytochalasin A inhibits secretion in *A. nidulans* (Torralba *et al*., 1998) and that a myosin I homologue, MYOA, plays some role in secretion in *A. nidulans* (McGoldrick *et al*., 1995). In our own cytochalasin A and latrunculin B washout experiments, we found that there was often rapid isotropic growth of hyphal tips after washout and before polarity was established (Figure 3, Supplemental Video5.mov and Video6.mov). These data together indicate that actin is important to the rate of exocytosis, not just the site of exocytosis.

Once secretory vesicles fuse with the plasma membrane and release their contents, excess membrane and components of the vesicle fusion machinery such as SYNA need to be recycled by endocytosis (Pelham, 1999; Fischer-Parton *et al*., 2000; Lewis *et al*., 2000; Read and Kalkman, 2003; Valdez-Taubas and Pelham, 2003). What are the sites of endocytosis at growing hyphal tips? In *S. cerevisiae*, there is compelling evidence that actin patches are sites of endocytosis, and there is a great deal of evidence that this is the case in *A. nidulans* as well. Araujo-Bazán *et al*. (2008) provide equally compelling evidence that the cortical actin/ABPA patches in *A. nidulans* contain the components of the endocytic machinery (including but not limited to ABPA). Endocytosis of the fluorescent membrane marker *N*-[3-triethylammoniumpropyl]-4-[*p*-diethylaminophenylhexatrienyl] pyridinium dibromide (FM4-64) requires actin (Penalva, 2005), and when FM4-64 is taken up, it initially localizes to organelles resembling actin patches. MYOA is important for endocytosis in *A. nidulans*, and GFP-MYOA localizes to cortical patches in vivo (Yamashita and May, 1998). Our data show that there is SYNA at the plasma membrane anterior to the actin/ABPA collar, but no SYNA at the plasma membrane posterior to the actin/ABPA collar. It follows that as the hypha grows SYNA is removed from the plasma membrane at the actin/ABPA collar.

Our data suggest a very obvious model for endocytosis and exocytosis at the growing tip. Exocytic vesicles fuse with the plasma membrane in a region anterior to the actin/ABPA collar (probably the region defined by SECC localization), releasing cell wall precursors. Vesicle components such as membrane and SYNA become incorporated into the plasma membrane. As the tip grows, the actin/ABPA collar moves forward and removes SYNA, membrane, and presumably other vesicle components from the plasma membrane by endocytosis. These components are then recycled. We suggest that the actin/ABPA patches posterior to the collar are involved in endocytosis for other purposes such as nutrient uptake.

Functions of Cytoskeletal Elements

Our data, in combination with published data cited above, indicate that actin has at least three functions in tip growth. First, as discussed, it is involved in exocytosis ahead of the actin/ABPA collar. This must involve the movement of exocytic vesicles and may involve the actual fusion of the vesicles with the plasma membrane. Second, it is required for endocytosis at the actin/ABPA patches. Third, it is involved in maintaining the structure of the tip growth complex.

Microtubules must also have at least three roles in tip growth, two of which may be closely related. The available evidence suggests that they are involved in long-range transport of vesicles to the hyphal tip region (Horio and Oakley, 2005, and other data discussed therein; Lenz *et al*., 2006). Note that there is considerable evidence that microtubules are extremely dynamic at the hyphal tip (Han *et al*., 2001; Szewczyk, Symeonidou-Sideris, and Oakley, unpublished data), continually growing and shrinking. They are thus not in stable contact with the Spitzenkörper and vesicles probably fall off of microtubules in the tip area more often than they are delivered directly to the Spitzenkörper. Microtubules are also required for the maintenance of directionality of tip growth because disassembly of microtubules leads to pronounced curvature of growth. Third, microtubules are required for keeping the tip growth apparatus in position at the tip. Over short periods, the tip growth apparatus generally stays at the tip, but without microtubules it often disappears from the tip and reforms elsewhere in the hyphal tip cell, correlating with, and presumably causing, formation of a lateral branch. Sometimes two or more lateral

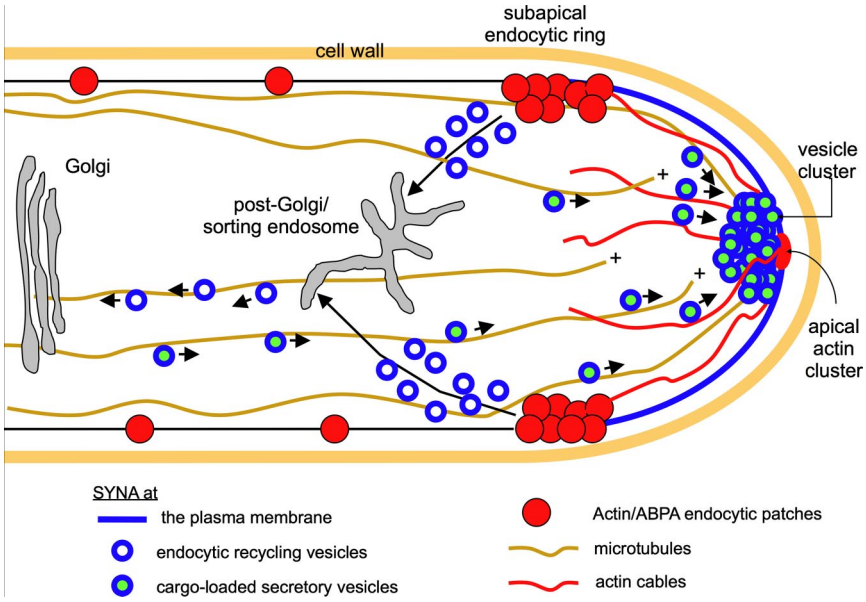

Figure 7. A model for tip growth in *A. nidulans*. The Spitzenkörper is not specifically labeled but includes (but is not necessarily limited to) the vesicle cluster and the apical actin cluster as well as the apical SSOA patch, SECC, and apical SEPA, which are not shown. Secretory vesicles containing components necessary for tip growth are transported toward the tip along microtubules powered by kinesin molecules (data not shown). The + ends of microtubules are extremely dynamic. In some cases, they transiently contact the vesicle cluster. In such cases, the secretory vesicles could be transferred directly from microtubules to the cluster. In other cases, secretory vesicles presumably fall off of the microtubule as the + end disassembles, and they are transported to the vesicle cluster by myosin molecules (not shown) on actin cables. Vesicles fuse with the plasma membrane, releasing their contents and the components of the membranes of the secretory vesicles (here represented by SYNA) become incorporated into the plasma membrane. As the tip grows, the ring of actin/ABPA endocytic patches moves forward, removing SYNA and other vesicle membrane components from the plasma membrane and incorporating them into endocytic vesicles for recycling. Although we do not have direct evidence, information from other systems and from Peñalva, Rodríguez and Arenza (personal communication) indicates that these vesicles move to the post-Golgi sorting endosome by mechanisms that are not yet defined. From this compartment, SYNA-containing membranes move away from the tip on microtubules, powered by dynein, to be eventually incorporated into Golgi-derived secretory vesicles containing cell wall biosynthetic enzymes and wall precursors.

branches form, each with their own tip growth apparatus. These findings are in keeping with previous findings that indicate that microtubules and associated motors are important for the directionality of growth and maintenance of the Spitzenkörper in *A. nidulans* and other filamentous fungi (Lehman, 1995; Riquelme *et al*., 2000, 2003; Konzack *et al*., 2005). Maintenance of direction of growth and position of the tip growth apparatus are probably aspects of the same function. Microtubules normally keep the tip growth apparatus in the correct position at the tip; thus, growth is more or less directional. Without microtubules, the tip growth apparatus can move off center causing curved growth or it can be displaced out of the hyphal tip area causing lateral growth.

An Integrated Model for Hyphal Tip Growth

Together, all of these data lead us to the following testable model (Figure 7). Secretory vesicles are transported by kinesins (including type 3 kinesins; Lenz *et al*., 2006) on microtubules to the tip region where they leave the microtubules and become associated with actin cables, the assembly of which is nucleated by the formin SEPA. Vesicles could fall off the microtubules and then become attached to myosin before moving along actin cables; alternatively, they could be transferred directly from microtubules to actin cables. We note that recent data on vertebrate myosin Va indicate that it is a wonderful candidate for transferring vesicles from microtubules to actin filaments (Ali *et al*., 2007). Vesicles are then moved on actin cables into a cluster at the Spitzenkörper where they are stored briefly before exocytosis, which occurs when vesicles are brought, perhaps on short actin cables, to the exocytotic complex at the apex. Exocytosis releases components required for the synthesis of new wall. SYNA (and, we presume, other components of the vesicular membrane) becomes incorporated into the plasma membrane during exocytosis. SYNA remains in the membrane until it is encountered by the forward moving actin/ABPA collar. It is then removed by endocytosis, recycled through endosomal and Golgi compartments and transported in a posterior direction on microtubules powered by dynein (Lenz *et al*., 2006).

ACKNOWLEDGMENTS

We thank C. Elizabeth Oakley for technical assistance and for proofreading the manuscript. This work was supported by a Deutsche Forschungsgemeinschaft fellowship to N.T.-T., Grant-in-Aid for Scientific Research 17570162 from Japan Society for the Promotion of Science (to T.H.), Dirección General de Investigación Científica y Tecnológica grants BIO2006-556 (to M.A.P.) and BFU2006-4185 (to E.A.E.), and National Institutes of Health grants GM-042564 (to S.A.O.) and GM-031837 (to B.R.O.). L.A.-B. is predoctoral fellow of the "Programa Nacional de Formación del Personal Investigador."

REFERENCES

Aalto, M. K., Ronne, H., and Keranen, S. (1993). Yeast syntaxins Sso1p and Sso2p belong to a family of related membrane proteins that function in vesicular transport. EMBO J. *12*, 4095–4104.

Ali, M. Y., Krementsova, E. B., Kennedy, G. G., Mahaffy, R., Pollard, T. D., Trybus, K. M., and Warshaw, D. M. (2007). Myosin Va maneuvers through actin intersections and diffuses along microtubules. Proc. Natl. Acad. Sci. USA *104*, 4332–4336.

Araujo-Bazán, L., Peñalva, M. A., and Espeso, E. A. (2008). Preferential localization of the endocytic internalization machinery to hyphal tips underlies polarization of the actin cytoskeleton in *Aspergillus nidulans*. Mol. Microbiol. *67*, 891–905.

Bartnicki-Garcia, S. (1990). Role of vesicles in apical growth and a new mathematical model of hyphal morphogenesis. In: Tip Growth in Plant and Fungal Cells, ed. I. B. Heath, San Diego, CA: Academic Press, 211–232.

Bartnicki-Garcia, S., Hergert, F., and Gierz, G. (1989). Computer simulation of fungal morphogenesis and the mathematical basis for hyphal (tip) growth. Protoplasma *153*, 46–57.

Bhatnagar, D., Yu, J., and Ehrlich, K. C. (2002). Toxins of filamentous fungi. Chem. Immunol. *81*, 167–206.

Brookman, J. L., and Denning, D. W. (2000). Molecular genetics in *Aspergillus fumigatus*. Curr. Opin. Microbiol. *3*, 468–474.

Cheng, J., Park, T. S., Fischl, A. S., and Ye, X. S. (2001). Cell cycle progression and cell polarity require sphingolipid biosynthesis in *Aspergillus nidulans*. Mol. Cell Biol. *21*, 6198–6209.

Cove, D. J. (1966). The induction and repression of nitrate reductase in the fungus *Aspergillus nidulans*. Biochim. Biophys. Acta *113*, 51–56.

David, D., Sundarababu, S., and Gerst, J. E. (1998). Involvement of long chain fatty acid elongation in the trafficking of secretory vesicles in yeast. J. Cell Biol. *143*, 1167–1182.

Engqvist-Goldstein, A. E., and Drubin, D. G. (2003). Actin assembly and endocytosis: from yeast to mammals. Annu. Rev. Cell Dev. Biol. *19*, 287–332.

Fidel, S., Doonan, J. H., and Morris, N. R. (1988). Aspergillus nidulans contains a single actin gene which has unique intron locations and encodes a gamma-actin. Gene *70*, 283–293.

Finger, F. P., Hughes, T. E., and Novick, P. (1998). Sec3p is a spatial landmark for polarized secretion in budding yeast. Cell *92*, 559–571.

Fischer-Parton, S., Parton, R. M., Hickey, P. C., Dijksterhuis, J., Atkinson, H. A., and Read, N. D. (2000). Confocal microscopy of FM4-64 as a tool for analysing endocytosis and vesicle trafficking in living fungal hyphae. J. Microsc. *198*, 246–259.

Gerst, J. E. (1997). Conserved alpha-helical segments on yeast homologs of the synaptobrevin/VAMP family of v-SNAREs mediate exocytic function. J. Biol. Chem. *272*, 16591–16598.

Gierz, G., and Bartnicki-Garcia, S. (2001). A three-dimensional model of fungal morphogenesis based on the vesicle supply center concept. J. Theor. Biol. *208*, 151–164.

Han, Gongshe, Liu, Bo, Zhang, Jun, Zuo, Wenqi, N., Morris, Ronald, and Xiang, X. (2001). The *Aspergillus* cytoplasmic dynein heavy chain and NUDF localize to microtubule ends and affect microtubule dynamics. Curr. Biol. *11*, 719–724.

Harris, S. D., Hamer, L., Sharpless, K. E., and Hamer, J. E. (1997). The *Aspergillus nidulans* sepA gene encodes an FH1/2 protein involved in cytokinesis and the maintenance of cellular polarity. EMBO J. *16*, 3474–3483.

Harris, S. D., Morrell, J. L., and Hamer, J. E. (1994). Identification and characterization of *Aspergillus nidulans* mutants defective in cytokinesis. Genetics *136*, 517–532.

Harris, S. D., Read, N. D., Roberson, R. W., Shaw, B., Seiler, S., Plamann, M., and Momany, M. (2005). Polarisome meets Spitzenkorper: microscopy, genetics, and genomics converge. Eukaryot. Cell *4*, 225–229.

Hohmann-Marriott, M. F., Uchida, M., van de Meene, A. M., Garret, M., Hjelm, B. E., Kokoori, S., and Roberson, R. W. (2006). Application of electron tomography to fungal ultrastructure studies. New Phytol. *172*, 208–220.

Horio, T., and Oakley, B. R. (2005). The role of microtubules in rapid hyphal tip growth of *Aspergillus nidulans*. Mol. Biol. Cell *16*, 918–926.

Huckaba, T. M., Gay, A. C., Pantalena, L. F., Yang, H. C., and Pon, L. A. (2004). Live cell imaging of the assembly, disassembly, and actin cable-dependent movement of endosomes and actin patches in the budding yeast, *Saccharomyces cerevisiae*. J. Cell Biol. *167*, 519–530.

Kaksonen, M., Sun, Y., and Drubin, D. G. (2003). A pathway for association of receptors, adaptors, and actin during endocytic internalization. Cell *115*, 475–487.

Kaksonen, M., Toret, C. P., and Drubin, D. G. (2005). A modular design for the clathrin- and actin-mediated endocytosis machinery. Cell *123*, 305–320.

Konzack, S., Rischitor, P. E., Enke, C., and Fischer, R. (2005). The role of the kinesin motor KipA in microtubule organization and polarized growth of *Aspergillus nidulans*. Mol. Biol. Cell *16*, 497–506.

Latge, J. P. (2001). The pathobiology of *Aspergillus fumigatus*. Trends Microbiol. *9*, 382–389.

Lehman, R. (1995). Cell-cell signaling, microtubules, and the loss of symmetry in the *Drosophila* oocyte. Cell *83*, 353–356.

Lenz, J. H., Schuchardt, I., Straube, A., and Steinberg, G. (2006). A dynein loading zone for retrograde endosome motility at microtubule plus-ends. EMBO J. *25*, 2275–2286.

Lewis, M. J., Nichols, B. J., Prescianotto-Baschong, C., Riezman, H., and Pelham, H. R. (2000). Specific retrieval of the exocytic SNARE Snc1p from early yeast endosomes. Mol. Biol. Cell *11*, 23–38.

Li, S., Du, L., Yuen, G., and Harris, S. D. (2006). Distinct ceramide synthases regulate polarized growth in the filamentous fungus *Aspergillus nidulans*. Mol. Biol. Cell *17*, 1218–1227.

McGoldrick, C. A., Gruver, C., and May, G. S. (1995). *myoA* of *Aspergillus nidulans* encodes an essential myosin I required for secretion and polarized growth. J. Cell Biol. *128*, 577–587.

Momany, M. (2002). Polarity in filamentous fungi: establishment, maintenance and new axes. Curr. Opin. Microbiol. *5*, 580–585.

Nayak, T., Szewczyk, E., Oakley, C. E., Osmani, A., Ukil, L., Murray, S. L., Hynes, M. J., Osmani, S. A., and Oakley, B. R. (2006). A versatile and efficient gene-targeting system for *Aspergillus nidulans*. Genetics *172*, 1557–1566.

Oakley, B. R., and Morris, N. R. (1981). A β-tubulin mutation in *Aspergillus nidulans* that blocks microtubule function without blocking assembly. Cell *24*, 837–845.

Oakley, C. E., Weil, C. F., Kretz, P. L., and Oakley, R. B. (1987). Cloning of the *riboB* locus of *Aspergillus nidulans*. Gene *53*, 293–298.

Osmani, A. H., Oakley, B. R., and Osmani, S. A. (2006). Identification and analysis of essential *Aspergillus nidulans* genes using the heterokaryon rescue technique. Nat. Protoc. *1*, 2517–2526.

Pearson, C. L., Xu, K., Sharpless, K. E., and Harris, S. D. (2004). MesA, a novel fungal protein required for the stabilization of polarity axes in *Aspergillus nidulans*. Mol. Biol. Cell *15*, 3658–3672.

Pelham, H. R. (1999). SNAREs and the secretory pathway-lessons from yeast. Exp. Cell Res. *247*, 1–8.

Penalva, M. A. (2005). Tracing the endocytic pathway of *Aspergillus nidulans* with FM4–64. Fungal Genet. Biol. *42*, 963–975.

Protopopov, V., Govindan, B., Novick, P., and Gerst, J. E. (1993). Homologs of the synaptobrevin/VAMP family of synaptic vesicle proteins function on the late secretory pathway in *S. cerevisiae*. Cell *74*, 855–861.

Read, N. D., and Kalkman, E. R. (2003). Does endocytosis occur in fungal hyphae? Fungal Genet. Biol. *39*, 199–203.

Riquelme, M., Bartnicki-Garcia, S., Gonzalez-Prieto, J. M., Sanchez-Leon, E., Verdin-Ramos, J. A., Beltran-Aguilar, A., and Freitag, M. (2007). Spitzenkorper localization and intracellular traffic of green fluorescent protein-labeled CHS-3 and CHS-6 chitin synthases in living hyphae of *Neurospora crassa*. Eukaryot. Cell *6*, 1853–1864.

Riquelme, M., Gierz, G., and Bartnicki-Garcia, S. (2000). Dynein and dynactin deficiencies affect the formation and function of the Spitzenkörper and distort hyphal morphogenesis of *Neurospora crassa*. Microbiology *146*, 1743–1752.

Riquelme, M., Fischer, R., and Bartnicki-Garcia, S. (2003). Apical growth and mitosis are independent processes in *Aspergillus nidulans*. Protoplasma *222*, 211–215.

Sharpless, K. E., and Harris, S. D. (2002). Functional characterization and localization of the *Aspergillus nidulans* formin SEPA. Mol. Biol. Cell *13*, 469–479.

Smith, M. G., Swamy, S. R., and Pon, L. A. (2001). The life cycle of actin patches in mating yeast. J. Cell Sci. *114*, 1505–1513.

Steinberg, G. (2007a). On the move: endosomes in fungal growth and pathogenicity. Nat. Rev. Microbiol. *5*, 309–316.

Steinberg, G. (2007b). Hyphal growth: a tale of motors, lipids and the Spitzenkorper. Eukaryot. Cell *6*, 351–360.

Sun, Y., Martin, A. C., and Drubin, D. G. (2006). Endocytic internalization in budding yeast requires coordinated actin nucleation and myosin motor activity. Dev. Cell. *11*, 33–46.

Szewczyk, E., Nayak, T., Oakley, C. E., Edgerton, H., Xiong, Y., Taheri-Talesh, N., Osmani, S. A., and Oakley, B. R. (2006). Fusion PCR and gene targeting in *Aspergillus nidulans*. Nat. Protoc. *1*, 3111–3120.

Torralba, S., Raudaskoski, M., Pedregosa, A. M., and Laborda, F. (1998). Effect of cytochalasin A on apical growth, actin cytoskeleton organization and enzyme secretion in *Aspergillus nidulans*. Microbiology *144*, 45–53.

Ungar, D., and Hughson, F. M. (2003). SNARE protein structure and function. Annu. Rev. Cell Dev. Biol. *19*, 493–517.

Valdez-Taubas, J., and Pelham, H. R. (2003). Slow diffusion of proteins in the yeast plasma membrane allows polarity to be maintained by endocytic cycling. Curr. Biol. *13*, 1636–1640.

Wedlich-Soldner, R., Bolker, M., Kahmann, R., and Steinberg, G. (2000). A putative endosomal t-SNARE links exo- and endocytosis in the phytopathogenic fungus *Ustilago maydis*. EMBO J. *19*, 1974–1986.

Yamashita, R. A., and May, G. S. (1998). Constitutive activation of endocytosis by mutation of myoA, the myosin I gene of *Aspergillus nidulans*. J. Biol. Chem. *273*, 14644–14648.

Yang, L., Ukil, L., Osmani, A., Nahm, F., Davies, J., De Souza, C. P., Dou, X., Perez-Balaguer, A., and Osmani, S. A. (2004). Rapid production of gene replacement constructs and generation of a green fluorescent protein-tagged centromeric marker in *Aspergillus nidulans*. Eukaryot. Cell *3*, 1359–1362.